Journal of Solid State Chemistry **155,** 86–95 (2000)
doi:10.1006/jssc.2000.8895, available online at http://www.idealibrary.com on IDEAL®

# Flux Additions in Barium Titanate: Overview and Prospects

Deep Prakash,* B. P. Sharma,* T. R. Rama Mohan,† and P. Gopalan†,[1]

*Powder Metallurgy Division, Bhabha Atomic Research Centre, Vashi Complex, Navi Mumbai 400 705, India; and †Department of Metallurgical Engineering and Materials Science, Indian Institute of Technology, Bombay, Powai, Mumbai 400 076, India

Received June 20, 2000; in revised form July 19, 2000; accepted July 27, 2000

DEDICATED TO PROFESSOR J. M. HONIG

**The existing literature on $BaTiO_3$ shows that the role of the various solid solutions and phases formed as a result of flux additions has not been addressed satisfactorily. In particular, their influence on the dielectric behavior of $BaTiO_3$ has been largely ignored. Thus, number of criteria for the choice of a flux material is discussed, and an overview of the various flux additives that have been used in $BaTiO_3$ is presented. In this work, the effect of $ZnO–B_2O_3$ and the $ZnO–WO_3$ fluxes on the dielectric characteristics is investigated and analyzed. Sufficient care is taken to address the effect of the various phases and solid solutions on the electrical and dielectric properties of $BaTiO_3$. A defect chemistry model is proposed and used to explain the observed electrical properties.** © 2000 Academic Press

*Key Words:* **dielectric constant; flux additions; $ZnO–B_2O_3$; $ZnO–WO_3$; $BaTiO_3$; sintering; dielectric loss; permittivity.**

## 1. INTRODUCTION

An increasing trend of miniaturization in the electronic industry calls for the development of high-charge storage capacity in a small volume of the capacitor. A high volumetric efficiency of the capacitor can be achieved by employing materials that possess a high dielectric constant. To date, various ceramic materials have been discovered that have dielectric constants covering a broad range between 30 and 30,000.

For a parallel-plate arrangement, considering the dimensions of a printed circuit board, the area between the electrodes works out to be typically 1–2 $cm^2$. An increase in capacitance then depends on minimization of the distance between the electrodes $d$, limited to $\sim$1 mm by practical considerations. Assembling the capacitors in parallel combination can further enhance the storage capacity of the device. Such a combination can also be devised by stacking alternate layers of ceramic tapes and conducting electrodes, and terminating them at the ends. This configuration is also known as the *multilayer ceramic capacitor* (MLCC).

Among known materials, barium titanate ($BaTiO_3$) is worthy of special mention, as it is the most widely utilized material for capacitor applications. The origin of the high dielectric constant (on the order of $10^3$) in $BaTiO_3$ stems from the presence of permanent electrical dipoles inherent to the crystal structure (1). However, the dielectric constant of barium titanate rises sharply with temperature, exhibiting a peak at the Curie point ($T_c = 130°C$), beyond which it falls hyperbolically, following the Curie–Weiss law (2). Since devices made from this material are to be used over a wide temperature range, pure barium titanate cannot be utilized for practical applications. It must be modified with various solid solutions and additives, giving rise to varying temp-e-rature behavior of ceramics, as per the application (3).

As mentioned earlier, the MLCC manufacturing consists of stacking alternate layers of ceramic tape and internal electrodes ink, which are cofired at the sintering temperature as $BaTiO_3$ (4). This cofiring is done in an oxidizing atmosphere, since sintering of titanates in a reducing atmosphere results in the reduction of $Ti^{4+}$ to $Ti^{3+}$, thereby increasing the dielectric loss and consequently deteriorating the dielectric properties (5). A constraint of maintaining high partial pressure of oxygen during cofiring necessitates the use of noble metal as a choice for an internal electrode. A Pd–Ag alloy is generally used for this purpose. However, the high cost of palladium, a constituent of the alloy, poses a major constraint in commercial usage.

One of the ways to reduce the cost of an internal electrode is to develop compositions that can be sintered in a reducing atmosphere, such that base metal electrodes, such as nickel, can be used. This may be achieved by suitably doping $BaTiO_3$ to prevent the reduction of $Ti^{4+}$ to $Ti^{3+}$ under low oxygen partial pressures. Another alternative would be to reduce the amount of Pd content in the alloy. The reduction in Pd content is directly related to optimizing the sintering behavior of the $BaTiO_3$-based compositions. Barium titanate-based ceramics are generally sintered at about 1350°C

[1] To whom correspondence should be addressed . E-mail: pgopalan@met.iitb.ernet.in.



0022-4596/00 $35.00

to achieve a dense material (6). These high sintering temp-eratures require the use of 70% Pd–30% Ag composition as the internal electrode. However, if the sintering temperatures can be reduced to 1150°C, an alloy containing 30% Pd–70% Ag would serve the purpose just as well, and considerable cost savings thus can be realized. In order to decrease the sintering temperature, addition of various types of sintering aids, mostly fluxes, has been attempted in recent years.

Much of the literature on flux sintering exists in the form of patents. Furthermore, an important area of research concerning the correlation between microstructure and dielectric property in flux sintered $BaTiO_3$ has been largely overlooked. Therefore, it is imperative to understand the effect of sintering aids on the densification and the correlation with dielectric properties, so that guidelines for realizing future commercial devices may be evolved.

Any flux material must satisfy a set of requirements. Primarily, other than lowering the sintering temperature, fluxing should not have any detrimental effect on the dielectric characteristics of the host material. The desirable dielectric properties include high dielectric constant, low dissipation factor, and an almost temperature-independent behavior of capacitance.

The first and foremost objective of the flux is to yield a high density following the sintering. A low sintered density is related to the presence of porosity in the microstructure, which not only dilutes the dielectric constant, but acts as a source for increasing the dielectric loss as well (7). Moreover, the presence of porosity also lowers the breakdown strength of ceramic material that are otherwise known for their utility in high-voltage applications.

In order to achieve a high dielectric constant in the sintered body, it is obvious that the material should be free from low-$k$ impurity and second phases. Addition of flux normally gives rise to second phases that may dilute the dielectric constant. In this regard, it is imperative to choose a flux so that the dilution of dielectric constant is kept at a minimum. Apart from the chemical composition, the amount and interaction of the flux with the parent matrix are also governing factors in the selection.

Dissipation factor or dielectric loss is the measure of energy loss from the device (3). The energy loss in the capacitor is exhibited by the heating effect, which is either due to ohmic conduction or nonohmic mechanism such as the vibration of dipoles (1). While the latter phenomenon depends on the basic crystal structure of the parent matrix, ohmic conduction can be minimized by suitably incorporating an insulating phase. Thus, an important characteristic of the added flux is that it should result in a low concentration of free charge carriers.

Another important feature of $BaTiO_3$-based materials is the temperature variation of the dielectric constant. This factor is strongly influenced by chemical as well as microstructural factors present in the ceramic material. A large grain size ceramic exhibits a sharp Curie peak, as compared to that with fine grains. Temperature compensation or flattening of temperature behavior has been attributed to the presence of a chemically inhomogeneous "grain core–grain shell" structure (7). An ideal fluxing agent should also influence all these chemical and microstructural features in order to yield a flattened permittivity–temperature response.

The criteria described above govern the choice of a suitable flux for $BaTiO_3$. Although practically it is difficult, if not impossible, to select an "ideal" flux fulfilling all the requirements, analyses of above factors often serve as a guideline in the choice of a flux. Some of the aspects such as dilution of the dielectric constant or temperature variation of the capacitance may be compromised, depending upon application of the material. A review on the existing literature in the following section reveals that the guidelines outlined above were not pursued in the past, but have rather emerged as a result of continuous endeavor toward development of better dielectric ceramics.

## 2. AN OVERVIEW OF FLUX ADDITIVES

Since only highly dense ceramics may be suitable for practical applications as devices, flux addition to $BaTiO_3$ started with the basic idea of achieving good densification at a lower temperature. The lowering of sintering temperatures to $\sim$1260°C by addition of small amounts of $SiO_2$ was discovered by Rase and Roy (8) as early as in 1955. However, their study mainly showed occurrence of liquid-phase sintering due to eutectic formation in the $BaTiO_3$–$SiO_2$ phase diagram. The electrical properties or the effect of liquid-phase sintering on the dielectric properties of barium titanate were not discussed; in fact, they did even not appear to signify much at that time.

As mentioned earlier, various types of fluxes for barium titanate have been discovered on date, which include many chemical compounds, glasses, low-melting oxides, fluorides, borates, silicates etc. In this section, a critical review of the various flux materials is presented. Since the discovery of fluxes was not confined to any particular class of compounds or any generic family, a chronological survey may not be appropriate. Instead, fluxes have been put into some broad categories, based on one major chemical constituent as follows.

### *Lithium Fluoride*

The addition of lithium fluoride (LiF) as flux to barium titanate was first reported by Walker *et al.* (9), who found that an addition of 0.5 to 3 wt.% of LiF aided densification of $BaTiO_3$ at a temperature much lower than that normally required for pure $BaTiO_3$. Following this, Amin *et al.* (10) and Anderson *et al.* (11) sintered $BaTiO_3$ with minor

additions of LiF at temperatures below 900°C, using long firing periods and obtained a material with improved dielectric properties. In another study, Haussonne *et al.* (12) reported the effect of 1–2 wt.% LiF addition on the sintering characteristics and dielectric properties. However, although sintering with LiF increased the dielectric constant at lower temperature and also improved the dissipation factor, prolonged heating resulted in substantial loss of Li as well as F. In order to overcome this, $BaLiF_3$ was used as a sintering aid, resulting in an improvement in the dielectric constant as well as dielectric loss characteristics (13). A gradual shift in the Curie peak toward room temperature was observed, attributed to the formation of a $BaTiO_3$–$BaLiF_3$ solid solution. A later study by Guha and Anderson (14) showed interaction of LiF with parent $BaTiO_3$ matrix. They showed an emergence of a liquid phase as early as 740°C and the formation of a $Li_2TiO_3$ compound at grain corners. However, no detailed correlation between microstructure and properties was presented.

### *Bismuth Oxide*

Flux based on bismuth oxide invented by Hanold (15) was described as a lead-free flux, consisting of 30–50% CdO and remaining $Bi_2O_3$. An addition of 5–40 wt.% flux to 95–60 wt.% base material gave rise to liquid-phase sintering at 1120°C. The resultant sintered ceramics had good temperature behavior (variation in capacitance 11–13% from $-55$ to $+125$°C) and low dielectric loss (0.8%). However, the dielectric constant was diluted, and the insulation resistance was also lowered. Hennings and Rosenstein (16) used an already prepared chemical compound $CdBi_2Nb_2O_9$ as a Bi-containing flux. This work highlighted the diffusion of Bi ion in the barium titanate lattice, which was eventually responsible for formation of complex perovskite phases and resulting in temperature-stable capacitors having a grain core–grain shell structure. However, prolonged heating gave rise to complete dissolution of Bi, resulting in a breakdown of the solid solution and the core–shell structure, thereby altering the temperature–permittivity response. In fact, this work showed that the temperature behavior of the sintered ceramics could be altered by controlling the extent of diffusion of Bi ions in the lattice. Recent work by Korumitsu *et al.* (17) also established $Bi_2O_3$–$B_2O_3$ flux as a sintering aid for $BaTiO_3$. However, they did not report the consequences of any prolonged heating.

### *Boron Oxide Fluxes*

Castelliz and Routil first reported the use of Boron oxide ($B_2O_3$) as a flux material for $BaTiO_3$ in 1969 (18). Since then, $B_2O_3$ has been increasingly used as a constituent for flux. This is probably due to the ability of $B_2O_3$ to form low-melting compounds with many oxides. Burn (19) has described $CdO$–$B_2O_3$ fluxes and their effect on the dielectric properties on $BaTiO_3$-based ceramics in detail. An addition of 4 wt.% flux having a composition of $2CdO.B_2O_3$ resulted in densification at 1100°C, accompanied by grain growth. Upon increasing the Cd/B ratio, excess CdO precipitated along the grain boundary, suppressing the grain growth as well as densification. An addition of bismuth oxide to this flux resulted in densification with a lower amount of flux, and also a higher Cd/B ratio was tolerated in the flux. It was also observed that Bi from the flux enters into the lattice. Burn suggested that Bi might occupy Ti as well as Ba sites in the lattice, depending on preparatory conditions. However, their study did not yield any information about the dielectric loss. Fluxes based on $ZnO$–$B_2O_3$ that lowered the sintering temperatures to 1100°C were also mentioned. However, once again, the effect of these fluxes on the dielectric behavior of $BaTiO_3$ was not investigated. Boron oxide fluxes, $B_2O_3$ and $PbB_2O_4$, were also investigated by Sarkar and Sharma (20), who reported liquid-phase sintering and improvement of dielectric strength. Flux compositions $CaO.2B_2O_3$ and $2CaO.Al_2O_3.2B_2O_3$ were added to $BaTiO_3$ by Armstrong *et al.* (21). This work showed that barium titanate compacts, added with fluxes up to 2 vol.% were sintered to nearly theoretical density at temperatures less than 1100°C. The flux compositions used in the study were congruently melted at 970 and 975°C, giving rise to an amorphous phase on cooling. Further addition of fine grain size monoclinic $ZrO_2$ to the fluxed $BaTiO_3$ acted as a grain-growth inhibitor. TEM analysis revealed a crystalline grain-boundary phase containing zirconia.

### *Glass Compositions*

One line of approach along where much of the work on flux sintering has taken place is the addition of small quantities of glass frit. The addition of a fluxing agent such as glass to $BaTiO_3$ is an effective method that enhances densification due to liquid-phase sintering at lower temperatures. As a result, numerous types of glasses have been developed as sintering aids for $BaTiO_3$. Matsuo *et al.* (22) have shown that 3–15 mol% addition of an eutectic mixture of $Al_2O_3$, $SiO_2$, and $TiO_2$ in a molar ratio of 4:9:3 lowered the sintering temperature to $\sim$1240°C. This flux addition also led to exaggerated grain growth that could be controlled by changing the heat treatment schedule (23). Boron oxide has also been used as a flux extensively, as it is a good glass former.

Glass compositions based on combinations of $Al_2O_3$, $SiO_2$, $TiO_2$, $B_2O_3$, etc., were attempted as fluxes, resulting in a number of patents (24–27). These compositions were based on borosilicate glasses that lowered the sintering temperatures to 1100°C, but could not prevent a decrease in the dielectric constant. Lead germanate compositions, studied by Payne and Park (28), showed that 33 vol.% addition of $(PbO)_x(GeO_2)_{y-z}(SiO_2)_z$ reduced the sintering temperature

to 750°C. On the other hand, 5–25 vol.% addition of $Pb_5Ge_3O_{11}$ resulted in a dielectric constant between 1000 and 1500. An improvement in the loss factor (0.01–0.02) was also observed (29).

However, glass-sintered $BaTiO_3$ may not always yield the desired dielectric properties. This is mainly due to presence of a continuous low-dielectric constant grain-boundary phase. In order to obtain materials with high dielectric constant, key steps appear to tailor the glass composition so as to promote densification with limited grain growth, and to reduce the volume fraction of second phases as well as porosity. Another important factor is to control diffusion into the parent titanate lattice. If the cations present in the glass substitute into the titanate lattice, the glass plays a dual role of flux and modifier. The extent of incorporation and distribution of the incorporated ions may shift the Curie peak, diffuse the sharpness of the transition, and change the volume fraction of second phases. The composition and the interaction between the flux and matrix are very important in characterizing, understanding, and controling the dielectric properties. Recent work on the interaction of glasses highlight this point (17, 30), which may be useful in designing microstructure-engineered capacitors.

*Other Fluxes*

Apart from the sintering aids mentioned above, CuO has been used by Hennings and Schreinemacher (31, 32). CuO-based fluxes have also been investigated by Yang (33). However, the use of these fluxes resulted in grain growth, and therefore a flattening of the Curie peak did not appear to be a possibility. Further, the dielectric loss for these flux additions has not been reported as yet.

A new emerging area appears to be the choice of relaxor-based materials as fluxes for barium titanate. Lead-based relaxor materials are known for high dielectric constant and broad Curie peak besides a lower sintering temperature (3). The use of relaxors may overcome the problem of dilution of dielectric constant, while simultaneously ensuring an enhanced densification. Furukawa *et al.* (34) have prepared stable ceramic dielectric composites by sintering a mixture of precalcined relaxor, $(Pb_{1-x}Sr_x)(Zn_{1/3}Nb_{2/3})_yTi_zO_3$, and prefired modified titanate, $Ba(Ti_{1-z}Zr_z)O_3$, at 1130°C. These composites have a dielectric constant between 2600 and 3700, and a variation in capacitance within $\pm 15\%$ between the temperature range $-55$ and 125°C. A similar approach has been suggested by Yamashita (35) and may be promising. However, it is fair to state that more work in this area is required.

Following the review on the various flux materials and the criteria described in the previous section for the choice of a flux, the objective of this work is to systematically investigate the role of ZnO-based binary flux systems. In particular, two compositions in the $ZnO–B_2O_3$ and one in the $ZnO–WO_3$ system have been chosen. The two compositions in the $ZnO–B_2O_3$ system correspond to the hypereutectic and eutectic points in the phase diagram (36). In light of the lack of correlation between the microstructure and dielectric behavior in the literature, sufficient care has been taken to address this aspect. Of particular interest in this work is understanding the role of the various phases on the sintering behavior and dielectric properties of $BaTiO_3$. Finally, defect chemistry is used to model the conductivity data.

## 3. EXPERIMENTAL WORK

Barium titanate powder used in this study was prepared by a conventional mixing and grinding process. Weighed amounts of high-purity barium carbonate and titanium dioxide powders were wet-mixed in a ball mill for 12 h, using high-purity alumina balls (5 mm diameter) as grinding medium. The mixed powder was calcined at 1100°C in air. Repeated grinding and calcination steps were carried out to ensure stoichiometric homogeneity in the product and a single-phase powder was obtained. Two flux compositions of the $ZnO–B_2O_3$ binary and one flux composition of $ZnO–WO_3$ were prepared separately. These fluxes were added to the conventionally prepared $BaTiO_3$, and the effect of their addition on the sintering behavior and dielectric properties was investigated. Table 1 shows the nomenclature of the fluxes and their compositions.

Flux (1) and flux (2) correspond to hypereutectic and eutectic compositions, respectively, in the $ZnO–B_2O_3$ system phase diagram (36). Binary $ZnO–B_2O_3$ fluxes were prepared by mixing weighed amounts of constituents in an agate mortar and pestle. An equivalent amount of boric acid was used in place of boron oxide. The mixed powders were prereacted at 300°C, ground, and mixed with the barium titanate powder. On the other hand, the $ZnO–WO_3$ flux was prepared by mixing the weighed constituents in mortar and pestle, followed by heating in a microwave oven. This resulted in a solid, friable mass that was ground and added to the $BaTiO_3$ powder for further study. The powder was compacted into pellets having 10 mm diameter and 2 mm thickness using a laboratory scale hand-operated hydraulic press. An addition of 1 wt.% PVA was made to impart green strength in the pellets. Sintering of pure $BaTiO_3$ was done in air at 1350°C, whereas flux-added pellets were sintered at different temperatures ranging from 1000 to

**TABLE 1**
**Fluxes and Compositions Used in the Study**

| Identification | Composition |
|---|---|
| Flux (1) | $ZnO–46$ mol% $B_2O_3$ |
| Flux (2) | $ZnO–32$ mol% $B_2O_3$ |
| Flux (3) | $ZnO–WO_3$ |

1250°C. Sintered pellets were lapped and coated with silver paste, and electrical contacts were soldered for measurement of their dielectric properties.

The powder and pellets were characterized for phase identification and phasic purity with a Philips analytical diffractometer employing Cu$K\alpha$ radiation. Particle size analysis of the powder was carried out using a Horiba-LA-500 laser diffraction particle size analyzer. Microstructural examination of sintered pellets was carried out using a Cambridge scanning electron microscope, model Stereoscan-240, and a JEOL-FX-2000 transmission electron microscope (TEM).

Electrical and dielectric properties were measured using a LCR meter SR-720 (Standard Research Systems, USA) as a function of frequency (100 Hz–100 kHz) in the temp-e-rature range between 25 and 150°C. Dimensional measurements of pellets were carried out using a TESA micrometer to an accuracy of $\pm$ 0.001 mm.

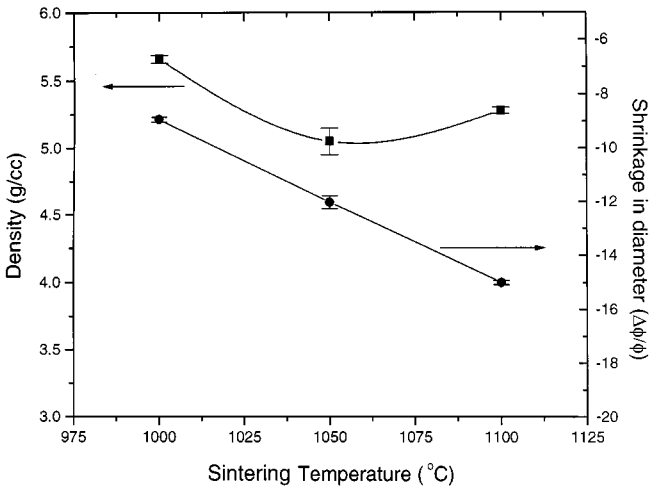


**FIG. 2.** Effect of sintering temperature on the density and shrinkage of $BaTiO_3$ sintered with flux (2).

## 4. RESULTS AND DISCUSSION

### *$ZnO$–$B_2O_3$ Fluxes*

X-ray diffraction (XRD) patterns of conventionally prepared powders indicated the formation of single-phase $BaTiO_3$. Particle size analysis showed a median of the particle size at 0.5 μm, and that all the particles were below 1 μm. Figures 1 and 2 exhibit the sintered densities and shrinkage in diameter of $BaTiO_3$ compacts sintered with addition of flux (1) and flux (2), respectively. For flux (1)-added ceramics, the increase in density and shrinkage was found to be linear with increase in the sintering temperature. On the other hand, the sintered density of flux (2)-added ceramics decreased and then increased marginally with an increase in sintering temperature. However, shrinkage in diameter was found to be linear in temperature. Further, conventionally prepared pure $BaTiO_3$ samples, which were sintered at 1350°C, were found to have a sintered density of 5.61 g/cc, comparable to that obtained for flux (1)-added samples at 1150°C. Therefore, the addition of flux, as expected, is found to lower the sintering temperature, attributed to liquid-phase sintering. In the $ZnO$–$B_2O_3$ phase diagram, a eutectic reaction occurs at 961°C (36). The composition of flux (1) used in this study corresponds to a liquidus temperature of 982°C. It is well known that a compatible liquid phase enhances densification (37). The small difference in the density of flux (1) and flux (2) compositions arises on account of the differing liquidus temperature as well as the viscosity of the liquid phase. In the present study, as expected, the presence of liquid phase increases the sintering rate.

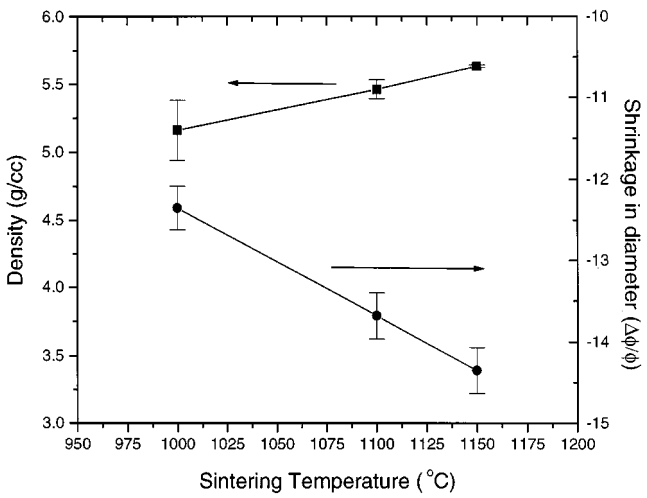


**FIG. 1.** Effect of sintering temperature on the density and shrinkage of $BaTiO_3$ sintered with flux (1).

In a separate study, densification behavior of a flux-assisted pellet was studied, and the activation energy for sintering estimated (38). In addition to a reduction in sintering temperature, the grain size of flux-added ceramics, sintered at 1150°C, was also reduced compared to that for pure $BaTiO_3$. A SEM photomicrograph of a conventionally prepared $BaTiO_3$ pellet and sintered at 1350°C is shown in Fig. 3a. The average grain size was nearly 5 μm, while some large grains with a size of 10 μm were also observed. Figure 3b shows a bright-field TEM micrograph of a flux (1)-sintered pellet, sintered at 1150°C. Submicron-size grains can be clearly noticed in the micrograph, which indicates an arrest of grain growth. Dielectric properties of flux-added and pure $BaTiO_3$ ceramics are shown in Figs. 4 and 5, respectively. The room temperature dielectric constant of flux-added ceramics increased with an increase in the sintering temperature. This may be attributed to the increase in the density. A higher porosity at a lower sintering temperature accounts for a dilution of the dielectric constant.

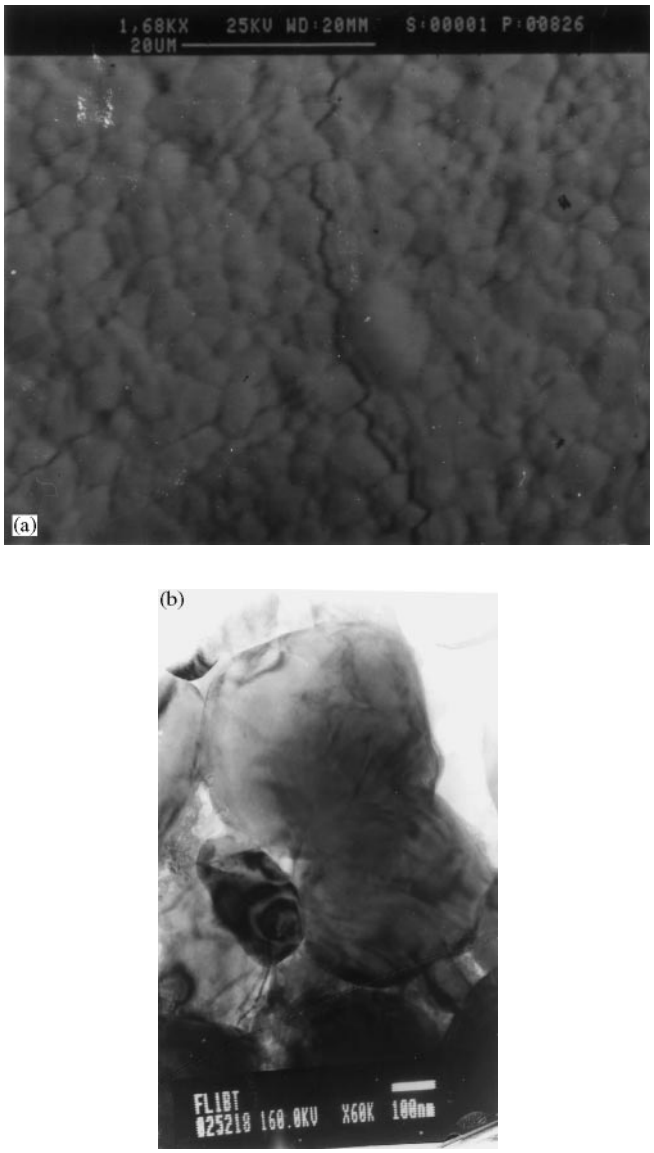


**FIG. 3.** (a) SEM photomicrograph of pure $BaTiO_3$ sintered at 1350°C. (b) Bright field TEM micrograph of flux (1)-added $BaTiO_3$ sintered at 1150°C.

The dielectric constant–frequency dependence, exhibited in Fig. 4, follows the Debye equations for dipole polarization for the lower frequency region ( $<120$ Hz), except for the pellets sintered at 1000°C. The increase in dielectric constant for 1000°C-sintered samples at lower frequencies may be due to a contribution from interfacial polarization. Figure 6 shows dielectric constant–temperature behavior for flux-added ceramics. The dielectric constant is higher for pellets sintered at higher temperatures, at all frequencies. This could be related to a lower porosity, as mentioned earlier. In addition, dielectric constants of flux-added ceramics were higher than that for pure $BaTiO_3$. This increase was attributed to a refinement of grain size (39). Also, the

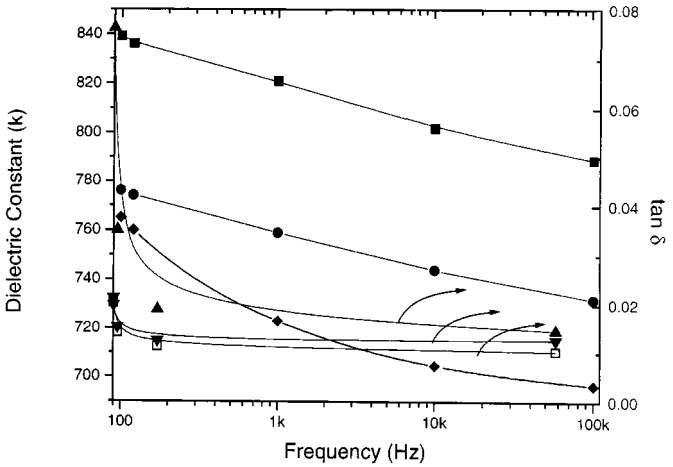


**FIG. 4.** Dielectric constant and dielectric loss as a function of frequency for flux-added samples sintered at different temperatures. Dielectric constant k at 1000°C (◆), 1100°C (●), 1150°C (■). Dielectric loss at 1000°C (▲), 1100°C (▼), 1150°C (□).

peak in permittivity that occurs at the Curie temperature was found at 130°C for all samples. This indicates that solid solution formation between the flux and the matrix did not occur. However, the interaction of liquid-phase resulted in a grain-boundary phase detected in XRD.

It must be noted that the resistivity–temperature behavior for flux-added ceramics was completely different from that for pure $BaTiO_3$. Figure 7 exhibits the resistivity–temperature curve for pellets sintered at 1000°C; the behavior for those sintered at other temperatures was similar. The temperature-independent resistivity values were almost an order of magnitude higher than that for pure $BaTiO_3$. Furthermore, the dielectric constants vs temperature curves in Fig. 6 do not exhibit a shifting of the Curie peak,

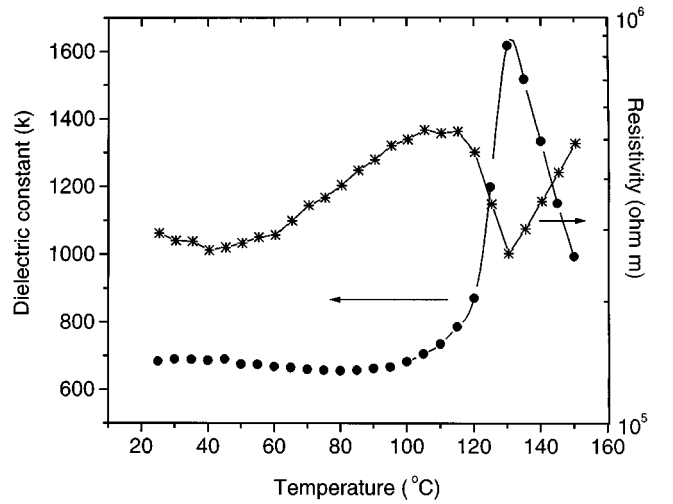


**FIG. 5.** Dielectric constant and resistivity as a function of temperature for conventionally prepared $BaTiO_3$ at 1 kHz.

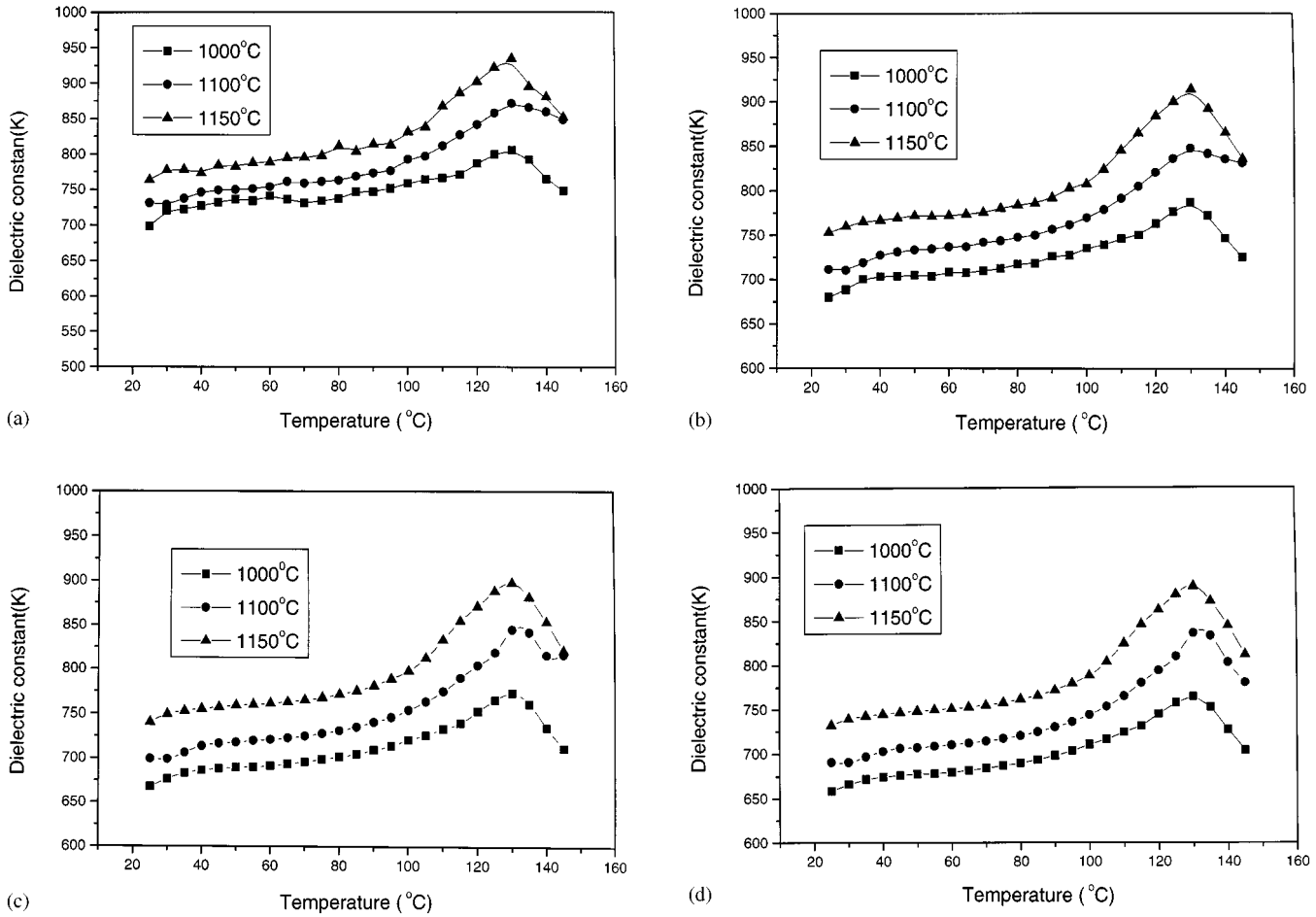


**FIG. 6.** (a) Dielectric constant vs temperature behavior at 100 Hz for flux (1)-added $BaTiO_3$ sintered at different temperatures. (b) Dielectric constant vs temperature behavior at 1 kHz for flux (1)-added $BaTiO_3$ sintered at different temperatures. (c) Dielectric constant vs temperature behavior at 10 kHz for flux (1)-added $BaTiO_3$ sintered at different temperatures. (d) Dielectric constant vs temperature behavior at 100 kHz for flux (1)-added $BaTiO_3$ sintered at different temperatures.

effectively ruling out the formation of a solid solution. This clearly indicates a presence of a second phase. Figure 8 exhibits a bright field TEM micrograph showing such a boundary phase at the triple-point grain corners as well as boundaries. The higher resistivity of the flux-sintered ceramics is attributed to this grain-boundary phase as that accounts for the only difference between the microstructure of pure and flux-assisted $BaTiO_3$. The structural details of this phase are presently being worked out.

### *$ZnO$–$WO_3$ Fluxes*

Pellets sintered with the addition of $ZnO$–$WO_3$, namely flux (3), were also investigated for sintering behavior and dielectric properties. Figure 9 exhibits the effect of sintering temperature on the density of flux (3)-added ceramics. The increase in density was rapid from 1175 to 1200°C. However, only a marginal increase was found for samples sintered at 1225°C. Further increase in the sintering temperature actually resulted in a slight decrease in the density.

This densification behavior may again be attributed to the liquid-phase sintering. An appearance of liquid phase during heating results in a rearrangement of particles and the density increases as a result of the filling of pores (37). Once the process saturates, on further heating, no appreciable enhancement of density is expected.

The phase diagram of $ZnO$–$WO_3$ shows congruent melting at 1210°C (40). Therefore, maximum densification should take place beyond this temperature. However, any deviation from the stoichiometry in the flux composition would result in a liquid-formation temperature away from the congruent melting temperature. The temperature at which the liquid phase starts appearing may be estimated from the phase diagram, depending upon whether the flux is hypo- or hyperstoichiometric. Also, the amount and composition of liquid can be assessed following the tie-line

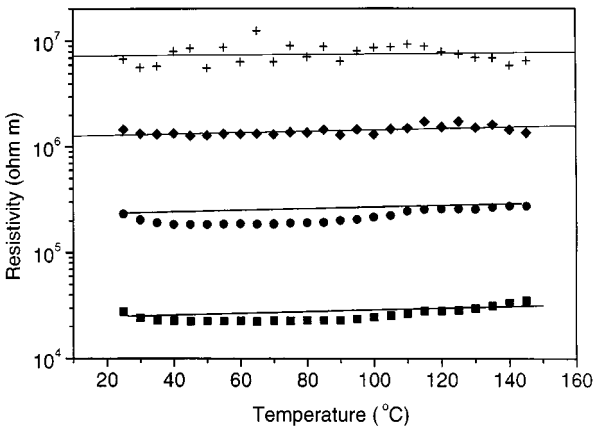


**FIG. 7.** Resistivity as a function of temperature for flux (1)-added $BaTiO_3$ at various frequencies, sintered at 1000°C (100 Hz ( + ), 1 kHz (◆), 10 kHz (●), 100 kHz (■)).

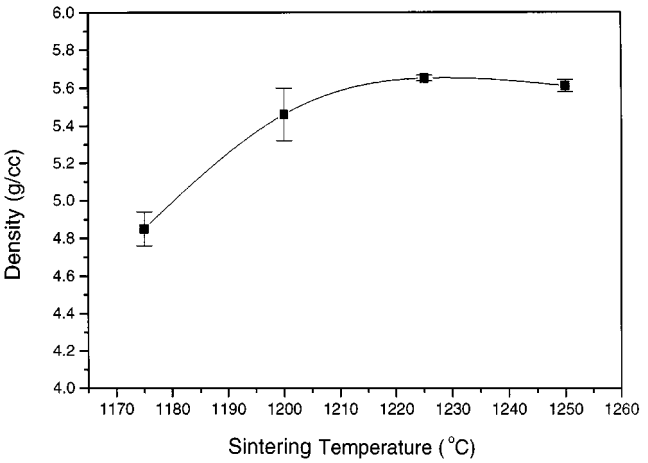


**FIG. 9.** Effect of sintering temperature on the density of flux (3)–added $BaTiO_3$.

approach, but is not deemed necessary for the present discussion. It must be noted that the liquidus temperature for both hypo- and hypereutectic compositions is below 1200°C. If small amounts of nonstoichiometric oxides were also present in the flux powder, the onset of densification would be at a temperature below 1200°C, explaining the observed behavior exhibited in Fig. 9. XRD investigations show a presence of certain phases, yet undetermined, that are formed due to interaction between liquid and the barium titanate grains.

Only the pellets sintered at 1250°C were characterized for dielectric properties. Figure 10 shows the room temperature dielectric constant as a function of frequency for sintered pellets. Beyond 1 kHz, the dielectric constant falls with an increase in frequency.

Figure 11 exhibits the variation of dielectric constant with temperature. The position of the Curie peak is clearly seen to be shifted to 35°C. This permittivity–temperature behavior may be attributed to the formation of a solid solution. Various elements present in the flux are known to form substitutional solid solution with perovskite compounds, replacing either the *A* or *B* site cations in the lattice.


**FIG. 8.** Bright field TEM micrograph of flux (1) sample sintered at 1000°C showing second phase at grain corner and along the boundary.

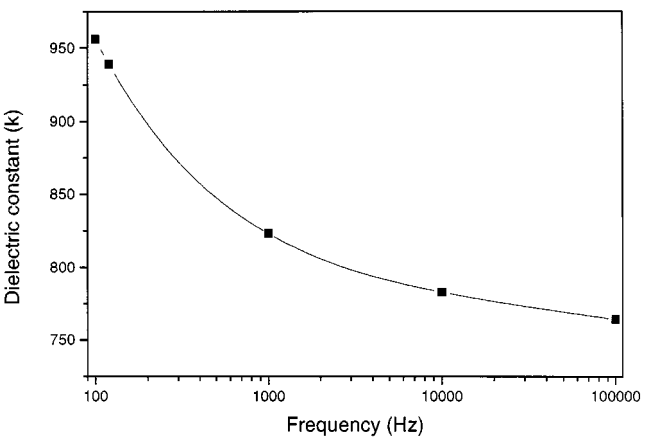


**FIG. 10.** Variation of room temperature dielectric constant as a function of frequency for $ZnO–WO_3$ (flux (3))-added $BaTiO_3$ sintered at 1250°C.

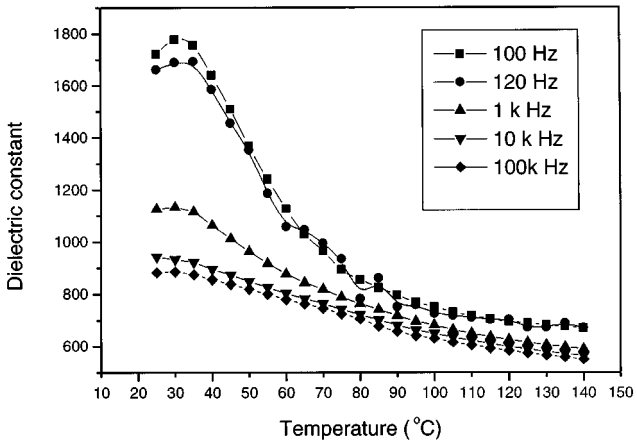


**FIG. 11.** Dielectric constant as a function of temperature at various frequencies for $ZnO–WO_3$ (Aux (3))-added $BaTiO_3$ sintered at 1250°C.

Whether an element would replace *A* or *B* cation generally depends on its ionic radius and coordination number. Tungsten is likely to replace $Ti^{4+}$ ions, resulting in a solid solution of the type $Ba(Ti_{1-x}W_x)O_3$. It is well known that a solid solution with $BaTiO_3$ results in a shifting of the Curie temperature (41, 42). In the present study, it is apparent that the solid solution with tungsten substituting for $Ti^{4+}$ is responsible for shifting the $T_c$ toward room temperature.

Figure 12 shows the resistivity–temperature curve for the flux (3)-added pellets. The resistivity starts increasing from 35°C and reaches a saturation value near 90°C. One of the striking feature of the curve is the PTCR (positive temperature coefficient of resistance) effect. The typical S curve is similar to that of $BaTiO_3$ reported in the literature, albeit with a lowering of the knee of the curve, which represents

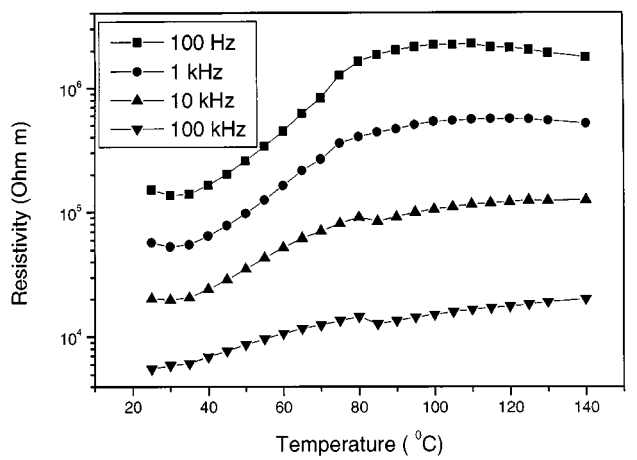


**FIG. 12.** Variation of resistivity as a function of temperature at several frequencies for flux (3)-added $BaTiO_3$, sintered at 1250°C.

the Curie temperature (43). However, the jump in resistivity was much less than that obtained for other donor-doped systems (44–47). The reason for this behavior is yet to be investigated. Further, W at the Ti site acts as a donor, $W_{Ti}^{\cdot}$ which may be compensated as per

$$2[W^{\cdot\cdot}] = n$$

or

$$[W^{\cdot\cdot}] = [V''_{Ba}].$$

In this model, the role of $Zn^{2+}$ is excluded, mainly on account of the inability of $Zn^{2+}$ to substitute for $Ti^{4+}$, the large variation between their ionic radii being responsible. The modeling of the conductivity data using the above defect model showed that the charge compensation mechanism in the flux (3)-added ceramics was due to formation of barium ion vacancies (41).

## 5. CONCLUSIONS

An addition of the $ZnO–B_2O_3$ flux to $BaTiO_3$ lowered the sintering temperature, attributing to liquid-phase sintering. However, average grain size was smaller than that of pure $BaTiO_3$. The refinement of grain size led to an improved dielectric constant. The dissipation factor, $\tan\delta$, which was due to the occurrence of a highly resistive grain-boundary phase, was also lowered.

Similarly, the addition of the $ZnO–WO_3$ flux was also found to lower the sintering temperature. However, the $ZnO–WO_3$ flux was also found to form a solid solution with the host matrix by replacing the *B* site cation. The dielectric constant–temperature curve for the $ZnO–WO_3$-added $BaTiO_3$ showed a shifting of the Curie peak toward room temperature. In addition, a PTCR effect, although not significant, was also observed. The resistivity values of the ceramics were modeled using defect chemistry, which showed that the charge compensation due to doping by donor tungsten results in the formation of barium ion vacancies.

## ACKNOWLEDGMENTS

This paper is dedicated to Professor J. M. Honig, who has retired after an illustrious and distinguished career at Purdue University. One of us (P.G.), who obtained a doctorate under the supervision of Professors J. M. Honig and J. Spałek, expresses his gratitude and respects to a great teacher and a thesis advisor, for having provided invaluable guidance at all times. His work ethic, dedication, and his contributions to further the understanding in the area of Solid State Chemistry in general, and oxide materials in particular, have and will always continue to be a source for inspiration.

The authors are thankful to Dr. K. R. Gurumurthy of the Atomic Fuels Division, BARC and Dr. G. K. Dey of Materials Science Division, BARC for their help in providing SEM and TEM facilities, respectively.

## REFERENCES


1. A. Chelkowski, "Dielectric Physics." Elsevier, New York, 1980.
2. Y. Xu, "Ferroelectric Materials and Their Applications." Elsevier, New York, 1991.
3. S. L. Swartz, *IEEE Trans. Elec. Ins.* **25,** 1 (1990).
4. C. P. Ward, *Brit. Ceram. Proc.* **41,** 85 (1989).
5. A. J. Moulson and J. M. Herbert, "Electroceramics," Chapman and Hall, London, 1990.
6. R. C. Buchanan (Ed.), "Ceramic Materials for Electronics," Dekker, New York, 1985.
7. N. Setter and E. L. Colla (Eds.), "Ferrroelectric Ceramics," Birkhausen, Verlag Basel, 1993.
8. D. E. Rase and R. Roy, *J. Am. Ceram. Soc.* **38,** 389 (1955).
9. B. E. Walker Jr., R. W. Rice, R. C. Pohanka, and J. R. Spann, *Am. Ceram. Soc. Bull.* **55,** 274 (1976); *Am. Ceram. Soc. Bull.* **55,** 284 (1976).
10. R. B. Amin, H. U. Anderson, and C. E. Hodgkins, US Patent No. 4,082,906 (1978).
11. H. U. Anderson, K. Atteberry, R. Amin, and C. Hodgkins, *Am. Ceram. Soc. Bull.* **58,** 368 (1979).
12. J. M. Haussonne, G. Desgardin, P. H. Bajolet, and B. Raveau, *J. Am. Ceram. Soc.* **66,** 801 (1983).
13. G. Desgardin, I. May, and B. Raveau, *Am. Ceram. Soc. Bull.* **64,** 563 (1985).
14. J. P. Guha and H. U. Anderson, *J. Am. Ceram. Soc.* **69,** 6192 (1986).
15. R. C. F. Hanold, U.S.Patent No. 4,081,857 (1978).
16. D. Hennings and G. Rosenstein, *J. Am. Ceram. Soc.* **67,** 249 (1984).
17. Y. Kuromitsu, S. F. Wang, S. Yashikawa, and R. E. Newnham, *J. Am. Ceram. Soc.* **77,** 493 (1994).
18. L. M. Castelliz and R. J. Routil, *Can. J. Ceram. Soc.* **38,** 69 (1969).
19. I. Burn, *J. Mater. Sci.* **17,** 1398 (1982).
20. S. K. Sarkar and M. L. Sharma, *Mater. Res. Bull.* **24,** 773 (1989).
21. T. R. Armstrong, K. A. Young, and R. C. Buchanan, *J. Am. Ceram. Soc.* **73,** 700 (1990).
22. Y. Matsuo, M. Fujimara, H. Sasaki, K. Nagase, and S. Hayakawa, *Am. Ceram. Soc. Bull.* **47,** 292 (1968).
23. Y. Matsuo and H. Sasaki, *J. Am. Ceram. Soc.* **54,** 471 (1971).
24. I. Burn, U.S.Patent No. 4,101,952 (1978).
25. G. H. Maher, U.S.Patent No. 4,066,426 (1978).
26. I. Burn, U.S.Patent No. 4,120,677 (1978).
27. I. Burn, U.S.Patent No. 4,283,753 (1981).
28. D. A. Payne and S. M. Park, U.S.Patent No. 4,218,723 (1979).
29. D. A. Payne and S. M. Park, U.S.Patent No. 4,158,219 (1979).
30. Y. Kuromitsu, S. F. Wang, S. Yashikawa, and R. E. Newnham, *J. Am. Ceram. Soc.* **77,** 852 (1994).
31. D. Hennings and H. Schreinemacher, U.S.Patent No. 4,222,885 (1980).
32. D. Hennings and H. Schreinemacher, U.S.Patent No. 4,244,830 (1981).
33. C.-F. Yang, *Ceram. Int.* **24,** 341 (1998).
34. O. Furukawa, M. Harata, M. Imai, Y. Yamashita, and S. Makaeda, *J. Mater. Sci.* **26,** 5838 (1991).
35. Y. Yamashita, *Am. Ceram. Soc. Bull.* **73,** 133 (1994).
36. "Phase Diagram for Ceramists," Vol. 1, p. 300. NRC, 1971.
37. R. M. German (Ed.), "Liquid Phase Sintering." Plenum Press, New York, 1989.
38. D. Prakash, B. P. Sharma, P. Gopalan, and T. R. Rama Mohan, paper presented at "International Conference on 'Advances in Powder Materials and Processing,' (POWMAT-99)," Hyderabad, India, 1999.
39. G. Arlt, D. Hennings, and G. deWith, *J. Appl. Phys.* **58,** 1619 (1985).
40. "Phase Diagram for Ceramists," Vol. 11, p. 9261, NRC, 1988.
41. Deep Prakash, B. P. Sharma, P. Gopalan, and T. R. Rama Mohan, unpublished work.
42. M. W. Barsoum, "Fundamentals of Ceramics." McGraw–Hill, New York, 1997.
43. G. V. Lewis and C. R. A. Cartlow, *J. Am. Ceram. Soc.* **68,** 555 (1985).
44. P. Padmini and T. R. N. Kutty, *J. Mater. Sci.: Mater. Elec.* **5,** 203 (1994).
45. J. Daniels and K. H. Herdtl, *Phil. Res. Rep.* **31,** 489 (1976).
46. H. Ihrig, *J. Am. Ceram. Soc.* **64,** 617 (1981).
47. J. Nowotny and M. Rekas, *Ceram. Int.* **20,** 257 (1994).